Electronic Supplementary Material (ESI) for Catalysis Science & Technology.

Supporting Information

Design the co-symbiotic Fe_xMn_yO catalysts for NO reduction by CO

Longqing Wei[a], Tangkang Liu[a], Yaohui Wu[a], Hao Liu[a], Lihui Dong[a,*], Bin Li[a]

[a] *Guangxi Key Laboratory of Petrochemical Resource Processing and Process Intensification Technology, School of Chemistry and Chemical Engineering, Guangxi University, Nanning 530004, PR. China*

*** Corresponding author:**
E-mail address: donglihui2005@126.com (L.H. Dong)
Postal address: 100# Daxue road, Guangxi University, Nanning 530004, Guangxi province, PR. China; Tel.: +86 0771-3233718; Fax: +86 0771-3233718.

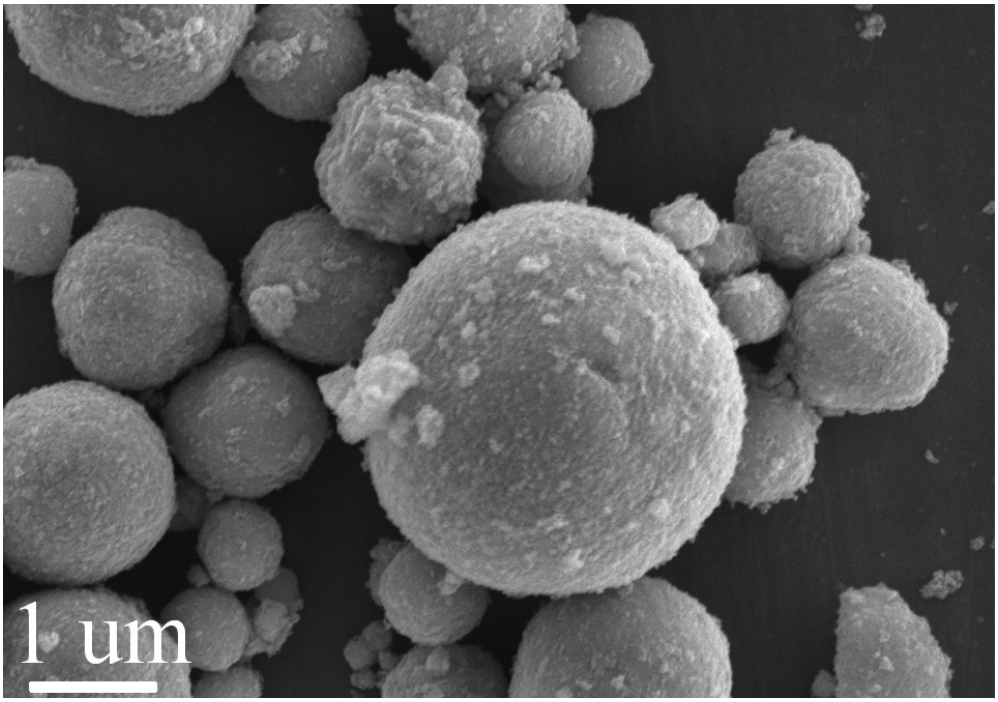

Fig. S1 SEM image of sample $Fe_{0.1}Mn_{0.9}O$

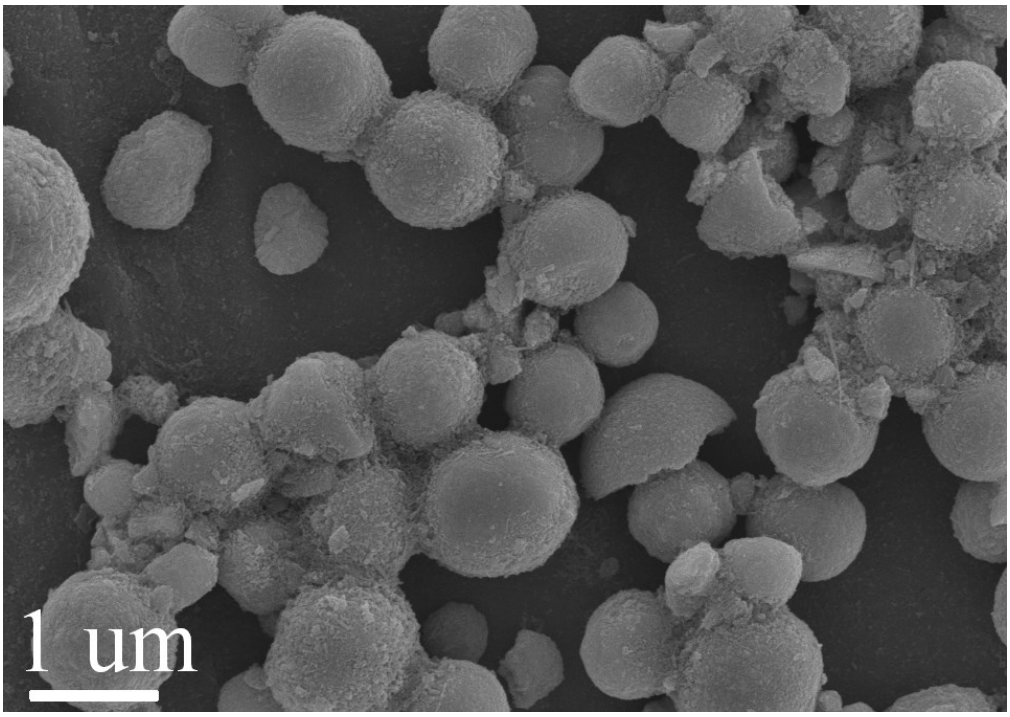

Fig. S2 SEM image of sample $Fe_{0.2}Mn_{0.8}O$

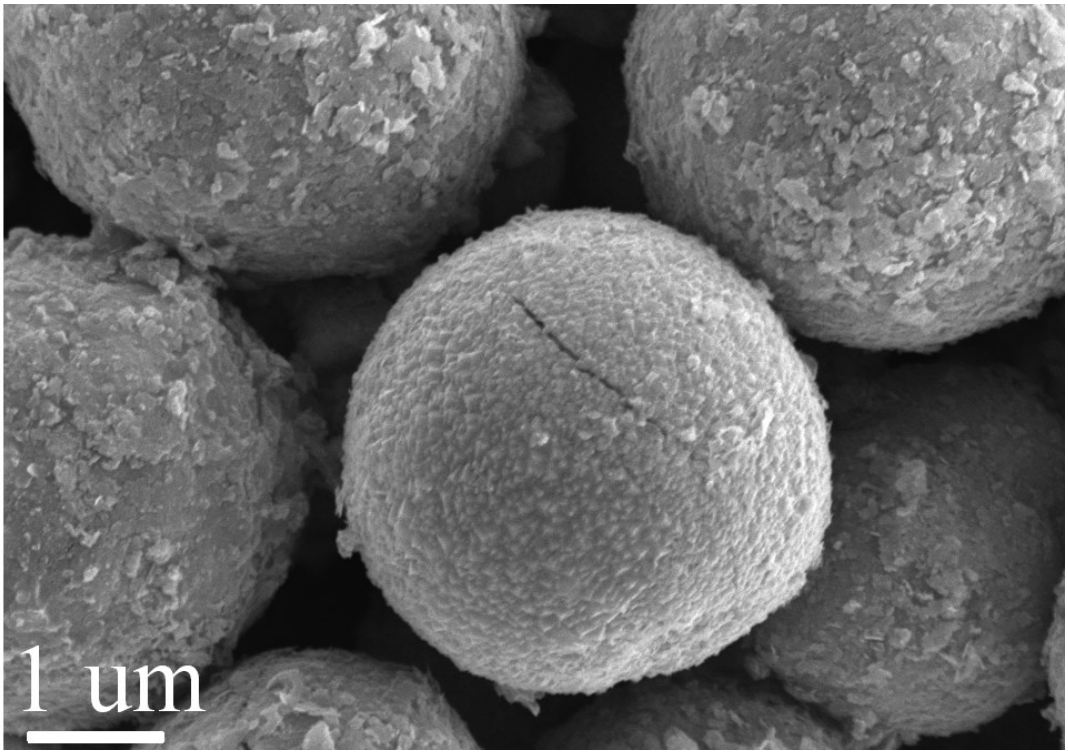

Fig. S3 SEM images of sample $Fe_{0.25}Mn_{0.75}O$

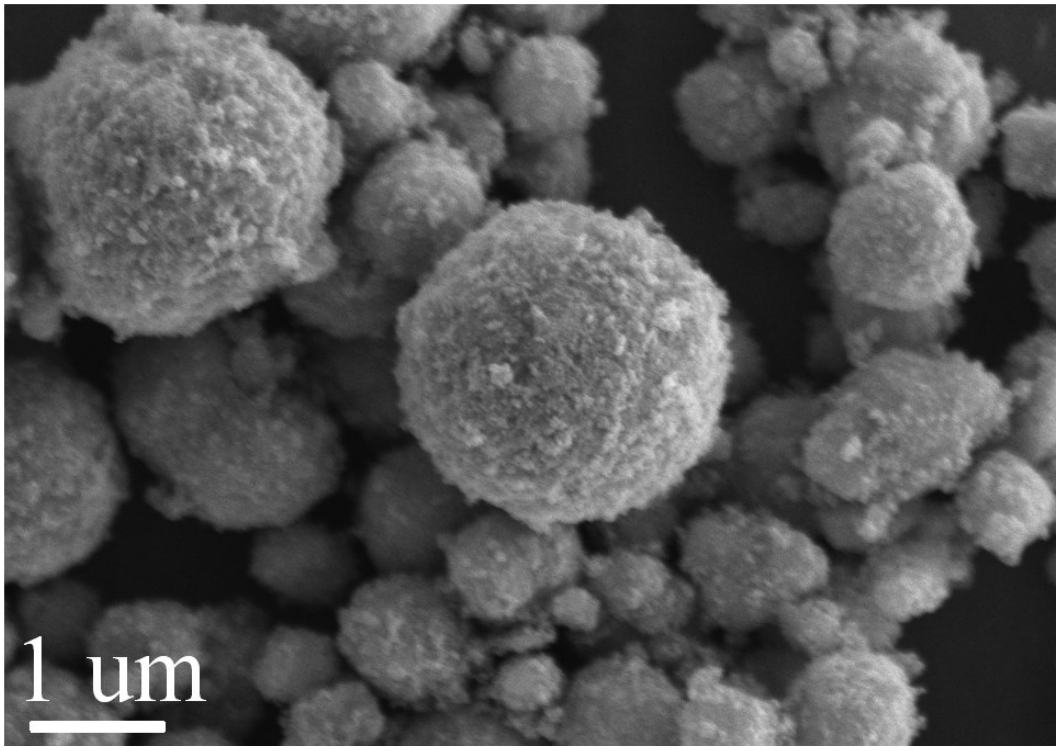

Fig. S4 SEM images of sample $Fe_{0.35}Mn_{0.65}O$

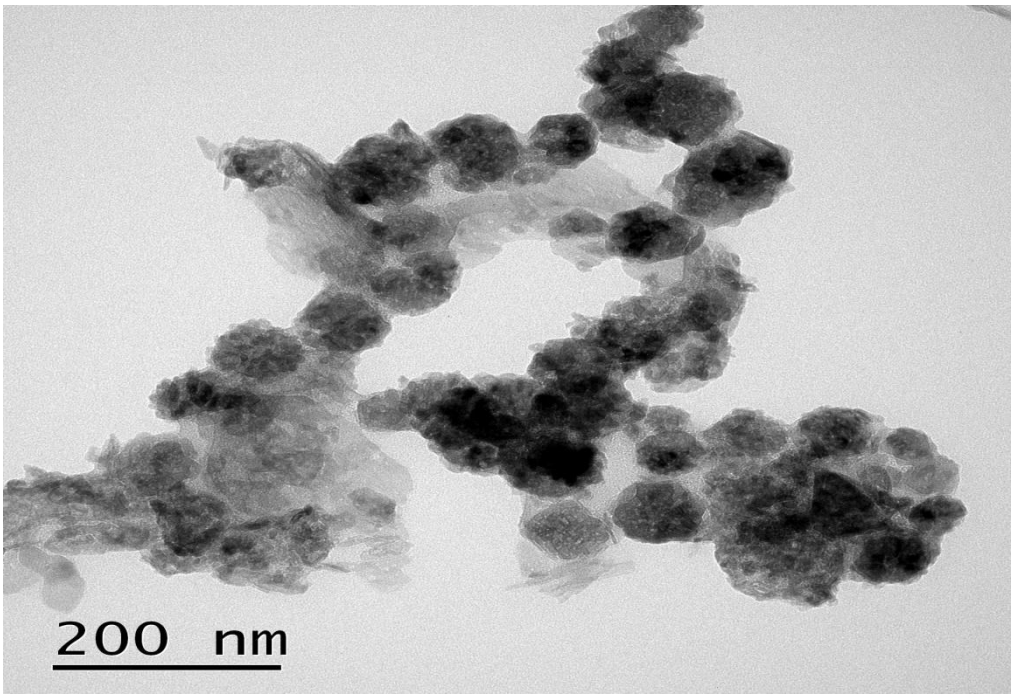

Fig. S5 the HRTEM image of $Fe_{0.3}Mn_{0.7}O$ at 200 nm

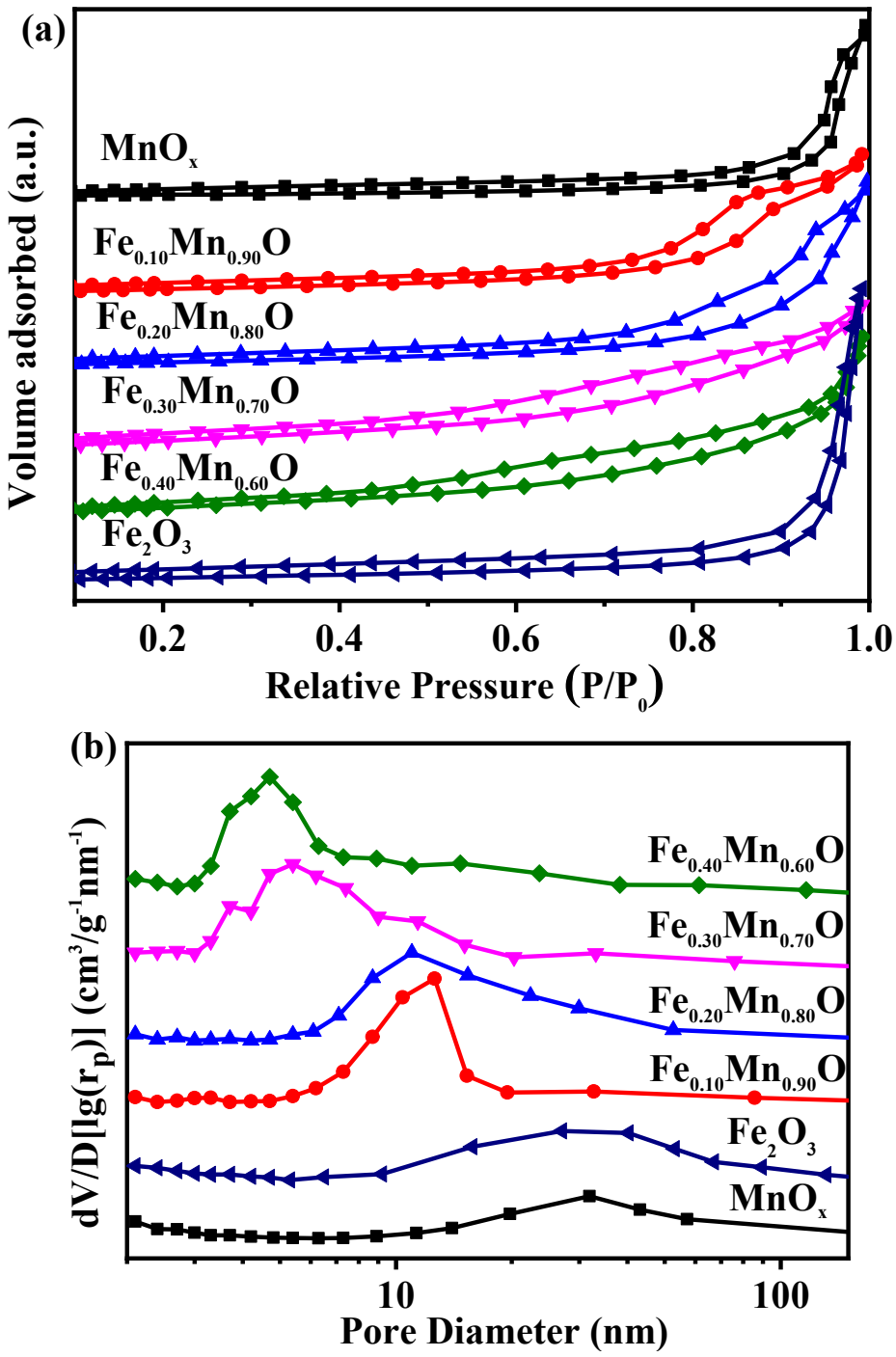

Fig. S6 the N_2 sorption isotherms and pore size distribution curves of Fe_xMn_yO samples.

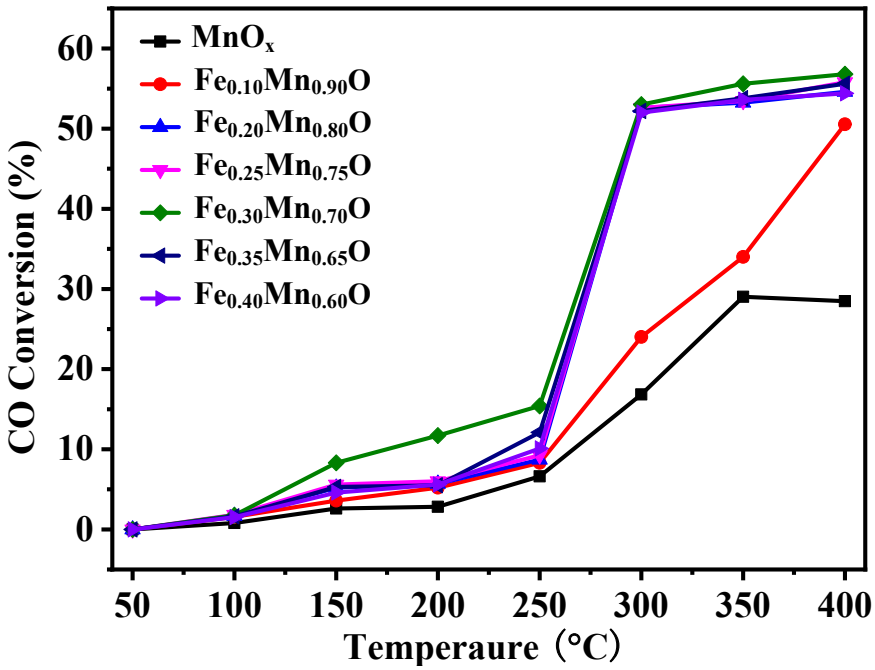

Fig. S7 the CO conversion of the Fe_xMn_yO catalysts. (Reaction condition: 50 mg of catalyst, 5 vol% NO/He+10 vol% CO/He, 1 bar, GHSV=24 000 $mL \cdot g_{cat}^{-1} \cdot h^{-1}$)

As can be seen from Fig. S7, the CO conversion rate was significantly increased after FeO_x was added. At low temperature, the CO conversion rate was about 15 %. With the temperature rising to 300 °C, the curve rose rapidly, which may be the result of the rapid adsorption and activation of the reaction gas on the catalyst at this temperature. At 300 ℃, the CO conversion rate reached 50 %, while the NO conversion rate reached 100 %, indicating that NO and CO were basically in dynamic equilibrium state on the catalyst. As the temperature rises further, it can be found that the CO conversion rate of the catalyst exceeds 50 %. This may be because the temperature rise leads to the reduction of the surface of the catalyst Fe_xMn_yO, which then leads to the CO conversion rate exceeding 50 %.

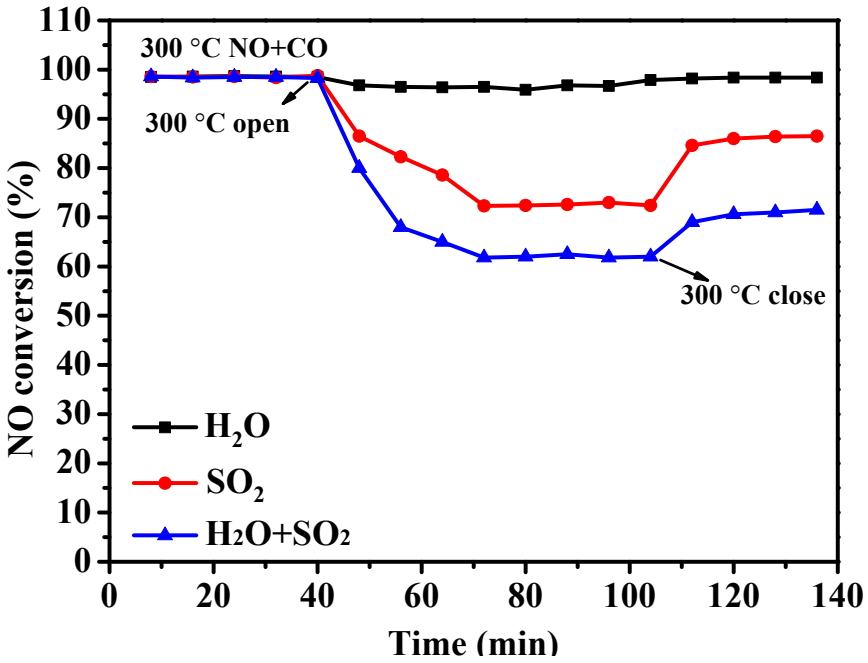

Fig. S8 The results of H_2O or/and SO_2 resistance test of the $Fe_{0.3}Mn_{0.7}O$ catalysts at 300 ℃ （10 vol% H_2O, 500 ppm SO_2 and 10 vol% H_2O + 500 ppm SO_2).

Fig. S8 is the test result of water resistance and sulfur resistance of $Fe_{0.3}Mn_{0.7}O$ catalyst at 300 °C. It can be seen from the figure that the NO conversion rate of the catalyst is basically unaffected after water is poured, indicating that the catalyst has good water resistance. When SO_2 is injected, NO conversion of the catalyst decreases obviously, but when SO_2 is shut down, NO conversion of the catalyst increases. When H_2O and SO_2 were injected simultaneously, the NO conversion rate of the catalyst showed the same trend as that of sulfur alone, but its decline was larger. This indicates that the influence of SO_2 on the catalyst is greater than that of H_2O, and the sulfur resistance of the catalyst is not very good. This may be due to the formation of sulfate on the surface of the catalyst by SO_2, which occupies the active part of the catalyst, leading to the degradation of the performance of the catalyst [6].

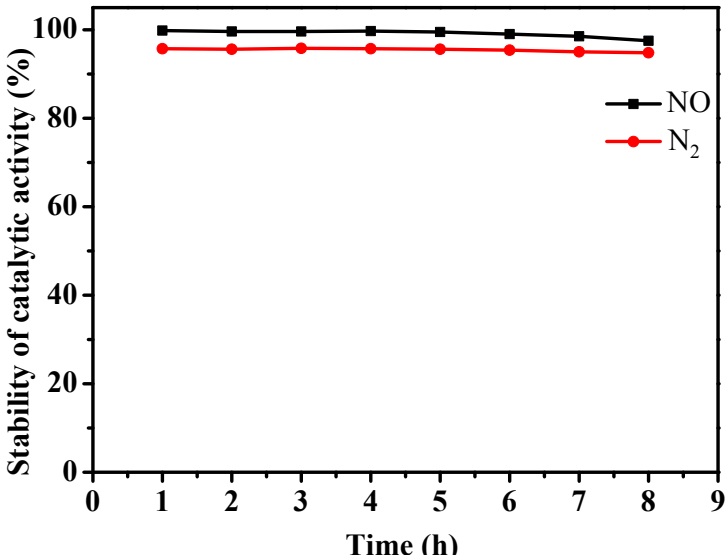

Fig. S9 The activity stability test of the $Fe_{0.3}Mn_{0.7}O$ catalysts at 300 ℃

(Reaction condition: 50 mg of catalyst, 5 vol% NO/He+10 vol% CO/He, 1 bar, GHSV=24 000 $mL \cdot g_{cat}^{-1} \cdot h^{-1}$)

The stability of the sample test data, are also supporting material supplement, specific content is as follows: the stability of the catalyst is the key factor in its catalytic application, so we passed in 300 ℃, the GHSV = 24 000 $mL \cdot g_{cat}^{-1} \cdot h^{-1}$ 8 hours pass into the CO-SCR reaction, can be found from figure integrated under 300 ℃ $Fe_{0.3}Mn_{0.7}O$ NO conversion and N_2 selectivity of catalysts basic did not change, only fell by about 2 %, this shows that the catalyst has good activity stability.

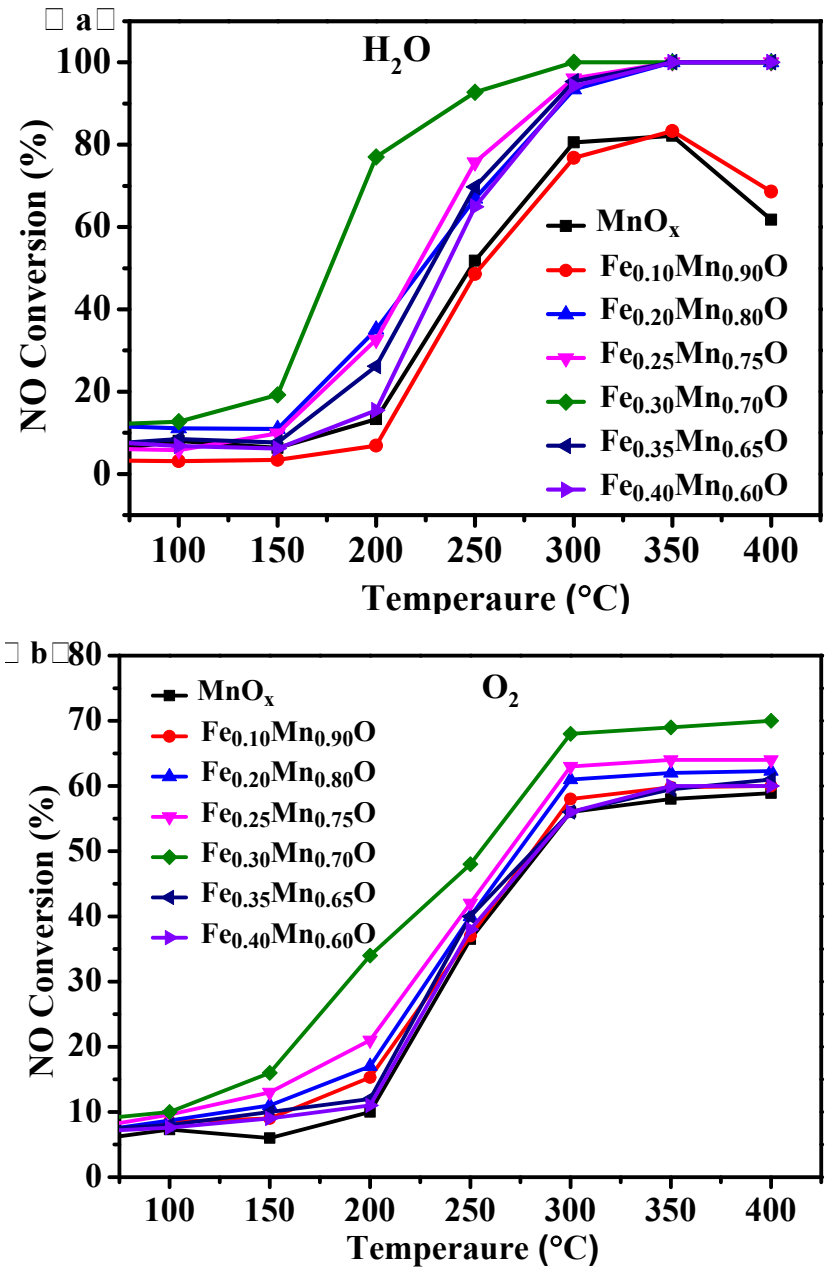

Fig. S10 The NO conversions in Fe_xMn_yO catalysts, reaction conditions: 10 vol. % CO (10 vol. % CO and 90 vol. % He), 5 vol. % NO (5 vol. % NO and 95 vol. % He) , 10 vol% H_2O(10 vol. % H_2O and 90 vol. % He), 1 vol. % O_2 (1 vol. % O_2 and 99 vol. % He), GHSV = 24000 $mL \cdot g_{cat}^{-1} \cdot h^{-1}$.

Catalytic property of these synthesized samples for NO_x reduction in presence of H_2O and O_2 are explored at 100–400 ºC, as observed in Fig. S10. It can be seen from Fig. S10(a) that the conversion rate of NO after adding water is basically unchanged, indicating that the water resistance of the catalyst is good. According to Fig. S10(b),

the optimal activity of all catalysts decreased significantly to about 65 % after O_2 was added, which indicated that the oxygen resistance of the catalyst was poor, and the addition of O_2 obviously inhibited the transformation of NO and reduced the NO conversion rate of the catalyst. However, it is worth noting that with the increase of temperature, the catalytic performance of catalyst $Fe_{0.3}Mn_{0.7}O$ still the best, which further proves that doping appropriate amount of Fe can effectively improve the performance of catalyst.However, the poor catalytic performance of the catalyst due to the addition of O_2 is also of concern. This is because our preparation Fe_xMn_yO catalyst is mainly applied to gasoline vehicles, a better general performance after oxygen catalyst is mainly used in diesel type of car, this is also a point, we should continue to further study for research that can have good oxygen resistance, and can be widely used in the gasoline cars of the catalyst.

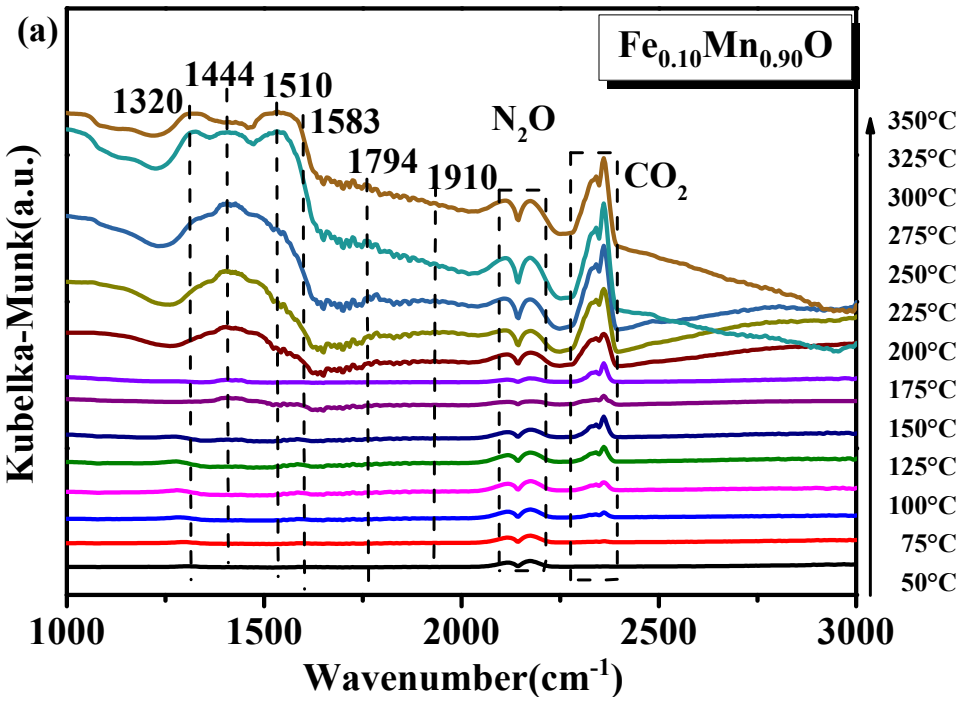
(a)
$Fe_{0.10}Mn_{0.90}O$
1320
1444
1510
1583
1794
1910
N_2O
CO_2
350°C
325°C
300°C
275°C
250°C
225°C
200°C
175°C
150°C
125°C
100°C
75°C
50°C
Kubelka-Munk(a.u.)
1000
1500
2000
2500
3000
Wavenumber(cm^{-1})

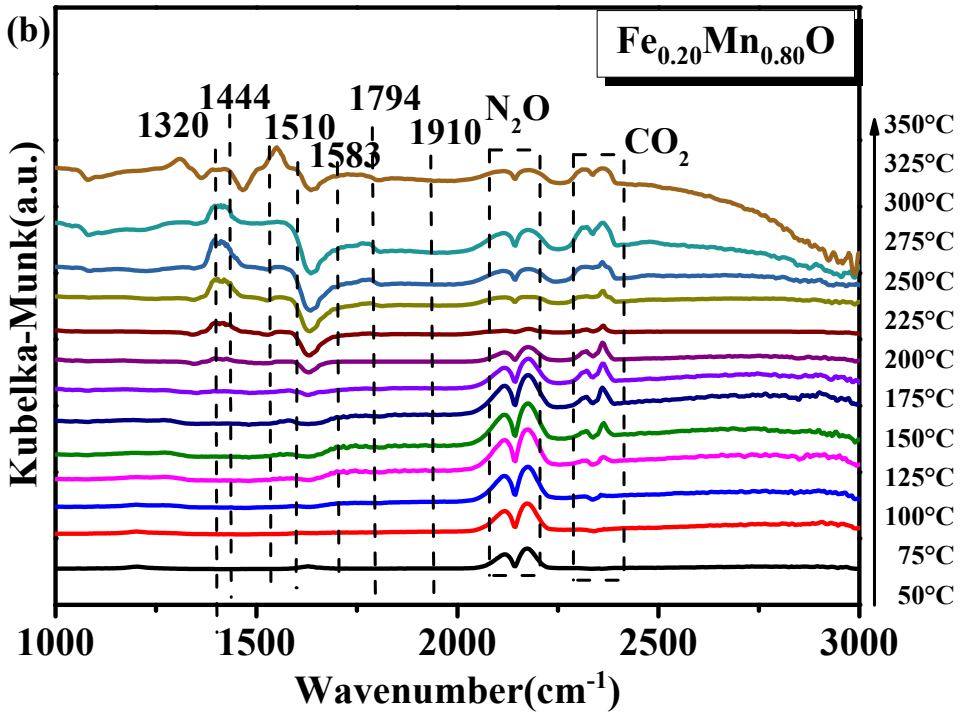
(b)
$Fe_{0.20}Mn_{0.80}O$
1320
1444
1510
1583
1794
1910
N_2O
CO_2
350°C
325°C
300°C
275°C
250°C
225°C
200°C
175°C
150°C
125°C
100°C
75°C
50°C
Kubelka-Munk(a.u.)
1000
1500
2000
2500
3000
Wavenumber(cm^{-1})

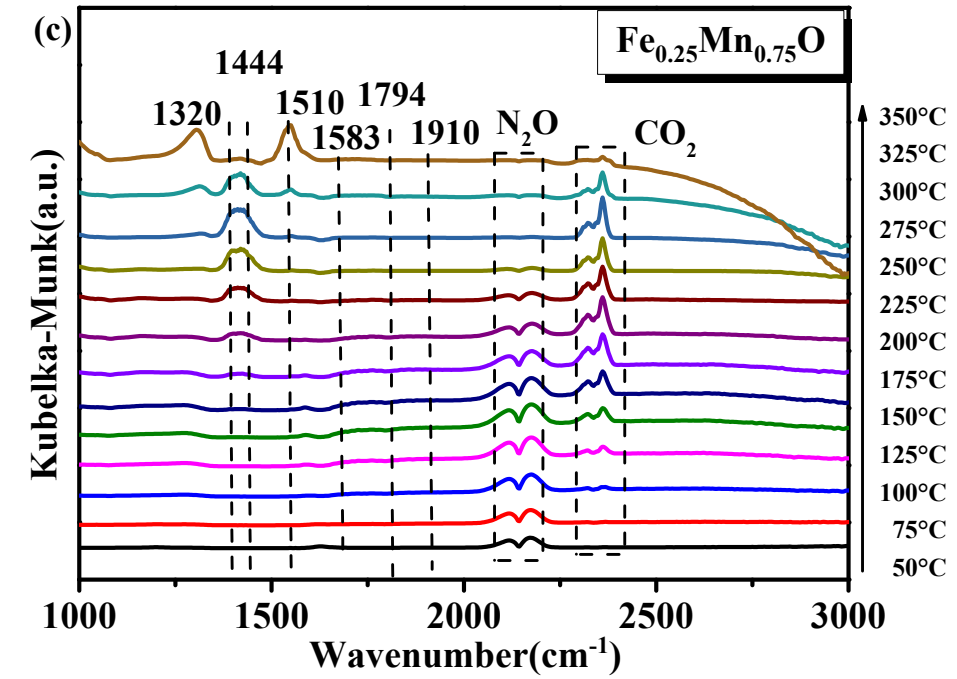
(c)
Fe0.25Mn0.75O
1444
1320
1510
1794
1583
1910
N2O
CO2
350°C
325°C
300°C
275°C
250°C
225°C
200°C
175°C
150°C
125°C
100°C
75°C
50°C
Kubelka-Munk(a.u.)
1000
1500
2000
2500
3000
Wavenumber(cm-1)

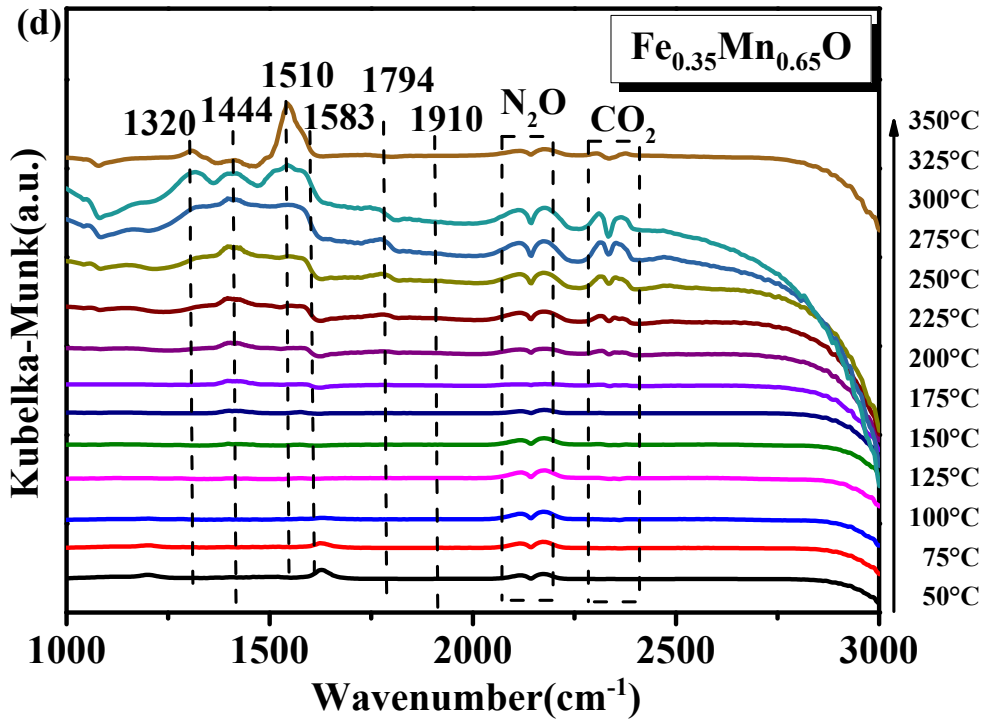
(d)
Fe0.35Mn0.65O
1510
1794
1320
1444
1583
1910
N2O
CO2
350°C
325°C
300°C
275°C
250°C
225°C
200°C
175°C
150°C
125°C
100°C
75°C
50°C
Kubelka-Munk(a.u.)
1000
1500
2000
2500
3000
Wavenumber(cm-1)

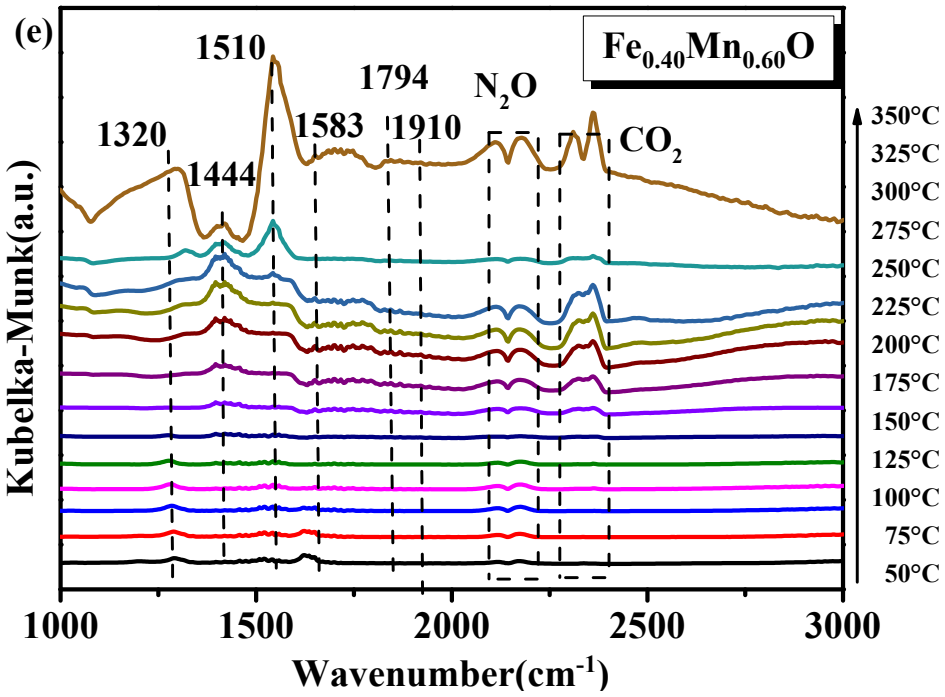

Fig. S11 the *in situ* DRIFTS spectra of NO (5.0 % in volume) + CO (10.0 % in volume) at different temperatures (a) $Fe_{0.1}Mn_{0.9}O$, (b) $Fe_{0.2}Mn_{0.8}O$, (c) $Fe_{0.25}Mn_{0.75}O$ (d) $Fe_{0.35}Mn_{0.65}O$, (e) $Fe_{0.4}Mn_{0.6}O$

Fig. S11 (a), (b), (c), (d), and (e) are respectively *in situ* DRIFTS spectra of NO+CO adsorption by catalyst $Fe_{0.1}Mn_{0.9}O$, $Fe_{0.2}Mn_{0.8O}$, $Fe_{0.25}Mn_{0.75}O$, $Fe_{0.35}Mn_{0.65}O$, $Fe_{0.4}Mn_{0.6}O$ at different temperatures. As can be seen from the Fig. S11, at lower temperatures (<100 ℃), according to the literature,[1-4] bridging bidentate nitrate (1583-1637 cm^{-1}), bidentate nitrate (1510-1543 cm^{-1}) and linear nitrite (1239-1513 cm^{-1}), NO gaseous peak (1849 and 1909 cm^{-1}), and infrared peak of N_2O absorption peak (2202 and 2238 cm^{-1}) appeared, but the peak of carbon adsorbent species is not detected. This indicates that NO_x preferentially adsorbs to the catalyst surface.[4, 5]

With the increase of temperature, NO species gradually decreased, indicating that the thermal stability of NO species in the catalytic reaction atmosphere is very poor. In addition, it can be seen that the infrared peaks of gaseous CO_2 (2337 and 2371 cm^{-1})

are enhanced as the temperature increases. This illustrates that the weak reaction of $CO + M^{n+} \rightarrow CO_2 + M^{(n-1)+}$ occurs under reaction atmosphere. On the other hand, this result also demonstrates that [O] species in $CO + [O] \rightarrow CO_2$ reaction are mainly stemmed from the transformation of $NO \rightarrow [O] + [N]$ rather than the reduction of high valence M^{n+} species. Therefore, we speculate that NO molecule is reacted preferentially with surface active O species to form NO_x species and surface oxygen vacancies (i.e. Fe^{x+}-□-Mn^{y+} species (x=2 or 3 and y=3 or 4)). With increasing the reaction temperature, the adsorbed NO_x species are increasingly dissociated into [N] and [O] over the Fe^{x+}-□-Mn^{y+} species, and then [N] is transferred into N_2 *via* reacting with other [N] and partial [O] reacts with CO into CO_2.[3] In addition, other [O] species convert to reactive oxygen species, activating NO molecules in the next catalytic cycle. This is consistent with the analysis conclusion in Fig. 9. Therefore, we explored the reaction mechanism of the catalyst in the original text according to the *in-situ* infrared results.

1. Experimental section

1.1. XRD characterization

XRD patterns of catalysts can be detected by X 'pert PRO at PANalytical. The XRD diffractometer uses a step length of 0.026, a residence time of 25.5 s per step, a scanning range of 5 °- 80 °, an excitation voltage of 40 KV, a tube current of 40 mA, and a scanning rate of 8 °·min^{-1}.

1.2. H_2-TPR characterization

H_2-TPR is performed by a FINESORB-3010 automated chemisorption apparatus (Finetec Corporation). For H_2-TPR, 0.025 g sample is placed in the sample tube, the temperature is programmed to 110 °C, and N_2 with a flow rate of 50 mL·min^{-1} was pretreated for 1 h. The water and weak adsorbed gas on the catalyst surface are purged and cooled to room temperature. The gas path is converted into H_2-Ar mixture with a flow rate of 10 mL·min^{-1} (H_2 with a distribution concentration of 7%), which is adsorbed for 30 min, so that the catalyst adsorption reached equilibrium, and then the heating rate of 10 °C·min^{-1} is increased from room temperature to the target temperature, and the curve of sample desorption of H_2 is collected by thermal conductivity detector (TCD).

1.3. O_2 - TPD characterization

O_2 - TPD is taking 0.1 g sample put in the sample tube, under 200 ℃ to the flow of 30 mL·min^{-1} He for pretreatment for 1 hour, then the cooling gas circuit to 10 mL·min^{-1} O_2 for adsorption, adsorption after 30 min, He (30 mL·min^{-1}) was used to purge the excess reaction gas in the gas channel. Purging 30 min, The O_2 desorption curves of samples are then collected with a thermal conductivity detector (TCD) from room temperature to target temperature at the rate of 10 ℃·min^{-1}.

1.4. in situ DRIFTS characterization

The Nicolet iS50 infrared spectrometer from Thermo Fisher is adopted, and the resolution of MCT detector is 4 cm^{-1}, and the scanning times are 32. For instantaneous reaction *in situ*, the proper amount of the sample is placed in the small fixed in the sample pool in the crucible, tong N_2 pretreatment for 1 hour under 350 ℃, cooling background spectra collected catalyst, then to test the adsorption intensity of reaction gas until the acquisition of the infrared spectrogram without too big change after, will switch to N_2 gas path, the temperature of the heating in the corresponding collection point catalyst response spectra. At last, the infrared diffuse reflection spectrum can be obtained by subtracting the background spectrum.

1.5. BET characterization

The adsorption−desorption isotherm of N_2 at 77 K is obtained using a Micrometrics TriStar I 3020 analyzer. The pore distribution and specific surface area are calculated from the nitrogen sorption isotherms by the Barrett−Joyner−Halenda and Brunauer−Emmett−Teller (BET) methods, respectively.

1.6. XPS characterization

The X-ray photoelectron spectroscopy (XPS) of the samples are obtained by using an ESCALAB 250Xi multifunctional imaging electron spectrometer (Thermo Fisher Company America), which used monochromatic Al Kα radiation (hν = 1486.6 eV) at the power level of 150 W. The electronic binding energy is calibrated on the basis of C 1s (284.8 eV). The irradiated area and detection depth of the samples are 2 mm × 1 mm and 2−5 nm, respectively.

1.7. SEM characterization

Scanning electron microscopy (SEM) measurements are performed with a HITACHI S-3400N electron microscope (Hitachi Company, Japan) at 20 kV. Samples for FESEM are suspended in ethanol and dispersed by ultrasonic, and then dropped onto an aluminium sheet.

1.8. TEM characterization

Transmission electron microscopy (TEM) images are taken on a Tecnai G2 F20 S-TWIN instrument (FEI Company, America) at an acceleration voltage of 200 kV.

References

1 L. Wang, M. Huang, B. Li, L. Dong, G. Jin, J. Gao, J. Ma, T. Liu, *Ceram Int.,* 2015, **41**, (10), 12988-12995.

2 C. Deng, Q. Huang, X. Zhu, Q. Hu, W. Su, J. Qian, L. Dong, B. Li, M. Fan, C. Liang, *Appl. Surf. Sci.,* 2016, **389**, 1033-1049.

3 T. Liu, Y. Yao, L. Wei, Z. Shi, L. Han, H. Yuan, B. Li, L. Dong, F. Wang, C. Sun, *J. Phys. Chem. C,* 2017, **121**, 12757-12770.

4 C. Deng, Q. Huang, X. Zhu, Q. Hu, W. Su, J. Qian, L. Dong, B. Li, M. Fan, C. Liang, *Appl. Surf. Sci.,* 2016, **389,** 1033-1049.

5 X. Lin, Y. Zhang, L. Yin, C. Chen, Y. Zhan, D. Li, *Int. J. Hydrogen Energy,* 2014, **39**, 6424-6432.

6 X. Shi, B. Chu, F. Wang, X. Wei, L. Teng, M. Fan, B. Li, L. Dong, L. Dong, *ACS Appl. Mater. Interfaces,* 2018, **10**, 40509-40522.